Dynamics and stability of hysteretic and multiphoton optical resonances of a single slightly relativistic cyclotron electron

Y. J. Ding and A. E. Kaplan

Department of Electrical and Computer Engineering, The Johns Hopkins University, Baltimore, Maryland 21218

Received November 9, 1988; accepted March 10, 1989

The stability of hysteretic cyclotron resonance, subharmonic optical excitation, and biharmonic optical cyclo-Raman resonances of a single electron is analyzed. A simple criterion of small-perturbation stability is derived whereby for the main resonance and subharmonic resonances those states are stable for which the derivative of the electron energy with respect to driving intensity is positive and vice versa. For the cyclo-Raman resonances in the absence of isolated states (the so-called isolas) the stability criterion is the same, whereas in the presence of the isolas it is reversed above the point of self-crossing in each isola. We also explored the behavior of the system in-large, using phase portraits and demonstrated existence of corridors of attraction as well as phase multistability in subharmonics and higher-order cyclo-Raman excitation.

I. INTRODUCTION

The interaction of microwave and optical radiation with a slightly relativistic single cyclotron electron precessing in a dc magnetic field can result in strong nonlinear-optical effects.[1–8] Even a slight relativistic change of mass of a single free electron[1,3] may result in the hysteretic cyclotron resonance[1–3,8] at the main frequency (observed recently in experiment[2]), i.e., in the situation when the driving frequency, Ω, is in the close vicinity of the unperturbed cyclotron frequency, Ω_0 [see Fig. 1(a)]. For the currently available dc magnetic fields the maximum cyclotron frequency is in the millimeter or submillimeter range. It was recently shown by us[4–8] that the strongly nonlinear cyclotron resonance can also be excited by *optical* pumping with a driving laser frequency (or frequencies) much higher than the cyclotron frequency. In particular, the single electron can exhibit high-order cyclotron subharmonics, in which case the ratio of driving (single) laser frequency to the frequency of cyclotron excitation is an integer, n [see Fig. 1(b)]. The subharmonics can be excited either in an almost synchrotron regime when only part of the electron orbit is illuminated by a very narrow laser beam[9] or in a "plane-wave" regime when the entire orbit of the electron is immersed in an optical beam.[5] It was also shown[4] that a strong cyclotron excitation can be obtained by *biharmonic* laser pumping when two laser frequencies, ω_1 and ω_2, differ by either Ω (e.g., $\omega_1 - \omega_2 = \Omega$) [see Fig. 1(c)] or 2Ω (i.e., $\omega_1 - \omega_2 = 2\Omega$). These effects may be regarded as a stimulated cyclo-Raman scattering of first and second orders. It is also feasible to observe cyclo-Raman excitation and scattering of an arbitrary nth order with the difference between the two driving laser frequencies being $\omega_1 - \omega_2 = n\Omega$, where n is an integer[7] [see Fig. 1(d)].

All the processes in consideration exhibit complicated nonlinear behavior, one of the main manifestations of which is multivalued solutions for steady-state regimes that result in such phenomena as hysteresis, bistability, and, in general, multistability of the amplitude as well as the phase. It is obvious that some of these steady states are stable, whereas others are unstable. The stability analysis is an important component of the theory of the phenomenon. Although the preliminary results indicating which of these states are stable and which are not have already been presented by us elsewhere,[1,3–8] the analysis itself has not been published yet. In this paper, we present the analysis of the transient regimes in the system for all the nonlinear processes mentioned above; it addresses both small-perturbation stability in the vicinity of the steady states and the behavior of the system in-large, i.e., when initial conditions are arbitrary (the so-called large perturbation). We also derive a simple criterion of steady-state stability for all the cases involved that is based on behavior of the electron energy versus driving intensity.

In our analysis we use a conventional envelope method assuming slowly varying amplitude and phase of cyclotron motion of the excited oscillations. Since the damping parameter of a free electron in a dc magnetic field (this parameter being related to very weak synchrotron radiation) is extremely small ($\Gamma \sim 10^{-11}$), the envelope approximation is valid with great margin. Our envelope equations were obtained using the general theory of nonlinear interaction of light with a single cyclotron electron.[3–8] This theory is based on the decomposition of the electron motion into a pure cyclotron component and noncyclotron components, the latter ones including all the higher-order oscillations with all possible frequency combinations. In order to treat all the different effects considered here from a unified point of view, we have also introduced a simplifying assumption that the center of cyclotron orbit is always at rest, i.e., we exclude from our consideration here the so-called magnetron and axial motion of the electron in a Penning trap. This is a legitimate approach if one wants to look into the most general patterns of the system behavior pertinent to all the different nonlinear processes in discussion. There is no doubt though that the further, more detailed theory of stability of nonlinear resonances will have to include other motions of

0740-3224/89/071299-07$02.00 © 1989 Optical Society of America

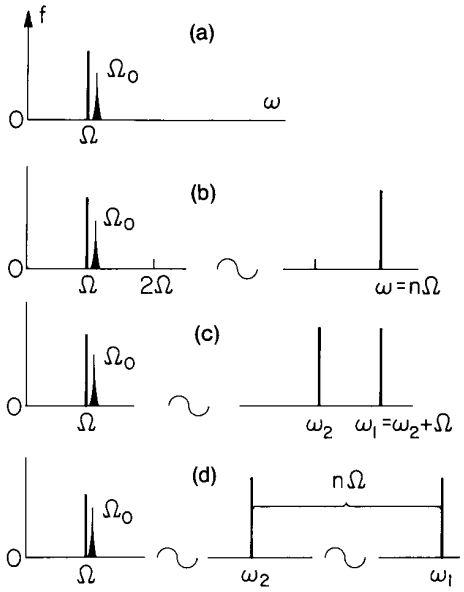

Fig. 1. Spectral arrangements of driving frequencies with respect to the unperturbed cyclotron frequency Ω_0 for (a) the main resonance at the frequency $\Omega \approx \Omega_0$, (b) the optical subharmonic resonance at the frequency $\omega/n \approx \Omega_0$, (c) the first-order cyclo-Raman resonance with the driving frequencies $\omega_1 - \omega_2 \approx \Omega_0$, and (d) the arbitrary order cyclo-Raman resonance with the driving frequencies $\omega_1 - \omega_2 \approx n\Omega_0$.

the electron, in particular, slow drift of the center of its orbit for a specific experimental configuration. It appears that this more specific approach will be more timely only when new experiments, especially those involving multiphoton resonances driven by biharmonic laser beams, will be designed.

The existence of stable states of the excited electron, especially in the case of high-order nonlinear excitation such as optical subharmonics and the optical cyclo-Raman effect, is significant for future experiments with laser excitation of cyclotron motion and for such physical applications of nonlinear cyclotron resonances as laser particle acceleration, phase optical bistability,[4,6] and coherent links between laser and microwave frequency standards using high-order subharmonics.[5,9]

Not surprisingly, the dynamic behavior of the electron motion exhibits a great deal of similarity to that of the nonlinear systems in a variety of fields, such as driven anharmonic oscillators[10,11] (in particular, the so-called Duffing oscillator, e.g., pendulum), the so-called nonlinear parametric systems,[12] and nonlinear circuits.[13,14] Similarly to the theory of most of these nonlinear systems, in order to show qualitatively the behavior of the system in-large, we use conventional two-dimensional phase portraits in which topological patterns of system behavior are displayed (in our case) in the space of spatial components of momentum.

This paper is structured as follows. In Section 2, we introduce the equation of motion and briefly review pertinent features of the general approach developed in Refs. 4–8. The dynamic behavior and stability analysis at the main cyclotron resonance, high-order subharmonics, and high-order cyclo-Raman excitation are discussed in Sections 3, 4, and 5, respectively.

2. EQUATIONS OF MOTION

Introducing the dimensionless variables defined in Refs. 3, 7, and 8 and assuming the cyclotron momentum of electron $\boldsymbol{\rho}$ in the form of[3,7,8]

$$\boldsymbol{\rho} = \rho[\hat{e}_x \sin(\Omega t + \phi) + \hat{e}_y \cos(\Omega t + \phi)], \tag{2.1}$$

where ρ and ϕ are the (unknown) slowly varying amplitude and phase of the cyclotron momentum, respectively, following the "hierarchical" procedure,[3,7,8] and introducing a complex variable $R = \rho e^{i\phi}$, we arrive at the equation governing dynamics of a cyclotron electron under action of driving fields:

$$dR/d\tau + R[\gamma - i(\gamma^{-1} - \Omega/\Omega_0)/\Gamma] = \mu\rho^{N-1}F(R, \rho), \qquad \rho = |R|, \tag{2.2}$$

where $\gamma = \sqrt{1 + \rho^2}$ is the dimensionless cyclotron electron energy; $\Gamma = 2e^2\Omega_0/3m_0c^3$ (Ref. 15) is the dimensionless linewidth, or damping parameter, of cyclotron resonance; $\tau = t/\tau_0$ is the dimensionless time, with $\tau_0 = 1/\Gamma\Omega_0$ being the relaxation time of the cyclotron electron; μ is the effective driving amplitude of the laser radiation for the respective nonlinear processes; $F(R, \rho)$ is a function, different for all three different nonlinear processes determined below for each of them; and N is the order of the nonlinear interaction. In the simplest case, i.e., at the main resonance, $\mu = 3c^2|E|/e\Omega_0^2$, $F = 1$, $N = 1$ where E is the amplitude of the electric field of the driving wave. The steady states of Eq. (2.2) correspond to $dR/d\tau = 0$. In the case of relatively small excitation ($\gamma - 1 \ll 1$) and frequency detuning ($|\Omega - \Omega_0| \ll \Omega_0$), Eq. (2.2) is reduced to

$$dR/d\tau + R[1 + i(\Delta + \rho^2/2)/\Gamma] = \mu\rho^{N-1}F, \tag{2.3}$$

where $\Delta = \Omega/\Omega_0 - 1$, which, for the case of the main resonance, coincides exactly with the envelope equation for a Duffing oscillator.[10] It is worthwhile to note that even a low-relativistic approximation allows one to obtain not only hysteretic resonance based on a small relativistic change of mass but also such complicated phenomena as subharmonics and cyclo-Raman excitation. The dynamics equations for the momentum amplitude ρ and ϕ follow immediately from Eq. (2.2):

$$d\rho/d\tau = -\gamma\rho + \Phi_\rho(\rho, \phi), \tag{2.4}$$

$$d\phi/d\tau = (\gamma^{-1} - \Omega/\Omega_0)/\Gamma + \rho^{-1}\Phi_\phi(\rho, \phi), \tag{2.5}$$

where $\Phi_\rho(\rho, \phi)$ and $\Phi_\phi(\rho, \phi)$ are, respectively, the real and imaginary parts of the term on the right-hand side of Eq. (2.2) multiplied by $e^{-i\phi}$ (Ref. 8) (see also below).

The stability of the steady states can be analyzed by examining the small-perturbation momentum amplitude $\Delta\rho$ and phase $\Delta\phi$ around the steady-state regimes $\rho = \rho_s$ and $\phi = \phi_s$, i.e.,

$$\rho = \rho_s + \Delta\rho, \qquad \phi = \phi_s + \Delta\phi. \tag{2.6}$$

Substituting ρ and ϕ in the form of Eqs. (2.6) either into Eq. (2.2) or into Eq. (2.3) and linearizing them with respect to small perturbations $\Delta\rho$ and $\Delta\phi$, we obtain the linear dynamic equations for $\Delta\rho$ and $\Delta\phi$ in the form

$$\Delta\dot{\rho} = a_{11}\Delta\rho + a_{12}\Delta\phi, \qquad \Delta\dot{\phi} = a_{21}\Delta\rho + a_{22}\Delta\phi, \tag{2.7}$$

with

$$a_{11} = \partial\Phi_\rho(\rho_s, \phi_s)/\partial\rho - (\gamma_s^2 + \rho_s^2)/\gamma_s,$$
$$a_{12} = \partial\Phi_\rho(\rho_s, \phi_s)/\partial\phi,$$
$$a_{21} = \partial[\rho_s^{-1}\Phi_\phi(\rho_s, \phi_s)]/\partial\rho - \rho_s\gamma_s^{-3}/\Gamma,$$
$$a_{22} = \rho_s^{-1}\partial\Phi_\phi(\rho_s, \phi_s)/\partial\phi. \tag{2.8}$$

It can be shown that in all the nonlinear processes discussed here the condition $a_{11} + a_{22} < 0$ is always satisfied. Therefore the stability of a steady state depends on the sign of the expression $a_{12}a_{21} - a_{11}a_{22}$. If the condition

$$a_{12}a_{21} - a_{11}a_{22} < 0 \tag{2.9}$$

is satisfied, the steady state corresponds to a stable (usually focal) point, whereas if the opposite condition is satisfied, the steady state corresponds to an unstable saddle point. The necessary condition for bifurcations (corresponding to the topologic changes in the phase portrait) to occur is $a_{12}a_{21} = a_{11}a_{22}$.

The specific results for the stability of all the steady states for all the processes in consideration will be discussed in the sections below. All these results, however, can be summarized in a criterion of small-perturbation stability based on the dependence of the energy of the steady state $\gamma_s = \sqrt{1 + \rho_s^2}$ (for all nonzero excitations, $\gamma_s > 1$) versus driving intensity μ^2. For the main resonance and for arbitrary order subharmonics, this criterion can be formulated in a simple form: If

$$d\gamma_s/d\mu^2 > 0 \tag{2.10}$$

the steady state is stable; if $d\gamma_s/d\mu^2 < 0$ it is unstable; i.e., those states are stable whose energy increases as the driving amplitude increases. This criterion is common for many physical systems; however, for some nonlinear excitations of a single electron it becomes reversed. Indeed, although for the cyclo-Raman processes condition (2.10) is still valid if the stable steady state is below the so-called self-crossing of each isola excitation, it reverses above the self-crossing of each isola excitation for the stable steady state (see Section 5 below).

The nonlinear dynamics of the nonlinear cyclotron motion in-large (i.e., for arbitrary initial perturbations) can readily be understood from the topology of the phase portrait, the equation for which is obtained by dividing Eq. (2.4) by Eq. (2.5) and thus eliminating time τ:

$$d\rho/d\phi = (-\gamma\rho + \Phi_\rho)/[(\gamma^{-1} - \Omega/\Omega_0)/\Gamma + \rho^{-1}\Phi_\phi]. \tag{2.11}$$

3. RELATIVISTICALLY HYSTERETIC CYCLOTRON RESONANCE AT THE MAIN FREQUENCY

Consider the hysteretic resonance at the main cyclotron frequency (i.e., when $\Omega \approx \Omega_c$, where Ω is the driving frequency and Ω_c is the cyclotron frequency of the excited electron) [see Fig. 1(a)]. The dynamics of ρ and ϕ are governed by Eq. (2.2) with[8]

$$\mu = 3c^2|E|/e\Omega_0^2, \quad F(R, \rho) = 1, \quad N = 1, \tag{3.1}$$

where E is the amplitude of the driving wave. The driving wave propagates parallel to the magnetic field $\mathbf{H}_0$ and is circularly polarized in such a way that the polarization vector precesses in the same direction as the electron does. In this case, Eq. (2.3) for low-relativistic excitation coincides exactly with the envelope equation for a Duffing oscillator[10]; therefore all the behavior patterns of a Duffing oscillator are expected to be manifested in a single-electron case, although the dynamics of energy γ will be altered as γ increases. Using the expressions for Φ_ρ and Φ_ϕ obtained from Eq. (3.1) as

$$\Phi_\rho = \mu\cos\phi, \qquad \Phi_\phi = -\mu\sin\phi, \tag{3.2}$$

the steady-state solutions for ρ and ϕ are determined from Eqs. (2.4) and (2.5) by the equations[1,3,8]

$$\rho_s = \mu[\gamma_s^2 + (\Omega/\Omega_0 - \gamma_s^{-1})^2/\Gamma^2]^{-1/2}, \tag{3.3}$$
$$\tan\phi_s = (\gamma_s^{-1} - \Omega/\Omega_0)/\Gamma\gamma_s; \tag{3.4}$$

see, e.g., Fig. 2(a). The small-perturbation stability of these steady states follows from Eqs. (2.7) with

$$a_{11} = -(\gamma_s + \rho_s^2\gamma_s^{-1}), \quad a_{12} = \rho_s(\Omega/\Omega_0 - \gamma_s^{-1})/\Gamma,$$
$$a_{21} = (\gamma_s^{-3} - \Omega/\Omega_0)/\rho_s\Gamma, \quad a_{22} = -\gamma_s. \tag{3.5}$$

One can show then from the stability criterion, condition (2.9), that for the fixed driving amplitude μ, the upper and lower amplitude branches are stable [see points s_1 and s_3 in part 1 of Fig. 2(a)] (they usually correspond to the focal points; see points 1 and 3 in Fig. 3); the middle branch between the upper and lower branches is unstable [see point u_2 in part 1 of Fig. 2(a)] (it corresponds to a saddle point; see point 2 in Fig. 3). It is readily shown from Eqs. (3.3) and (3.5) that $d\mu^2/d\gamma_s = -2\Gamma^2\gamma_s(a_{12}a_{21} - a_{11}a_{22})$. Therefore the criterion for the stable steady-state branch can be expressed as $d\gamma_s/d\mu^2 > 0$ ($\gamma_s > 1$); see parts 2 and 3 of Fig. 2(a), where

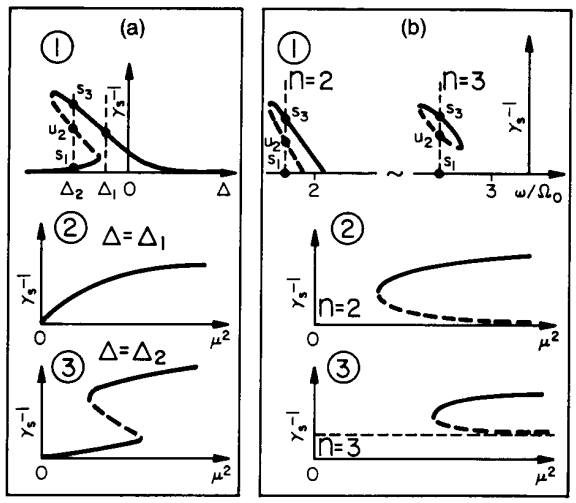

Fig. 2. Curves 1 illustrate the typical hysteretic steady-state excitation as a function of the driving frequency for the fixed driving amplitude; curves 2 and 3 illustrate the typical hysteretic steady-state excitation as a function of the driving amplitude for the fixed-frequency detunings (denoted by the respective vertical line) for (a) the main frequency resonance $\Omega \approx \Omega_0$ and (b) the optical subharmonic resonance $\omega \approx n\Omega_0$. In all cases the solid curves correspond to stable steady states and the dashed curves to unstable ones; the horizontal dashed line in part 3 of (b) corresponds to the lower limit of the excitation.

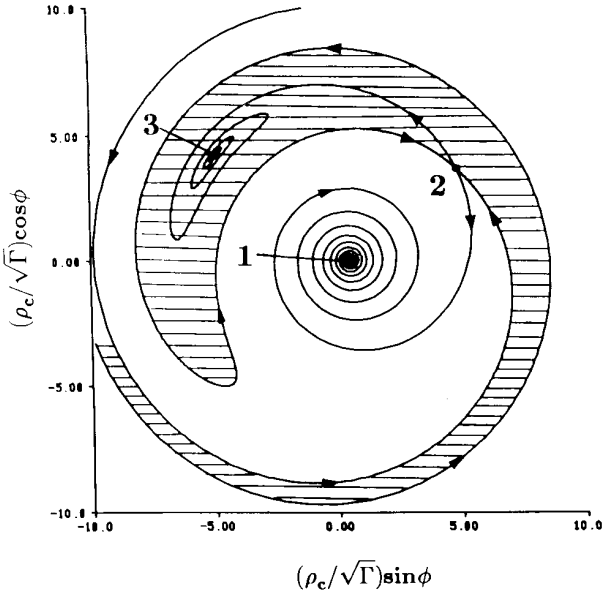

Fig. 3. Phase portrait for the main cyclotron resonance at the fixed driving amplitude $f = 10 \times \Gamma^{3/2}$ and the frequency detuning $\Omega/\Omega_0 - 1 = -20 \times \Gamma$. Points 1 and 3 correspond to the stable focal points; point 2 corresponds to the unstable saddle point. The hatched area corresponds to the narrow corridor for the stable state 3.

the solid curves correspond to stable states and the dashed curves to unstable states.

For the arbitrary initial conditions, i.e., for the behavior of the system in-large, the phase portraits can be obtained numerically from Eq. (2.11), with Φ_ρ and Φ_ϕ being expressed by Eqs. (3.2). The typical results are shown in Fig. 3, where the y component of the scaled cyclotron electron momentum $\rho_y' = (\rho/\sqrt{\Gamma})\cos\phi$ is depicted versus the x component of the scaled cyclotron electron momentum $\rho_x' = (\rho/\sqrt{\Gamma})\sin\phi$ for the fixed driving amplitude $\mu = 10 \times \Gamma^{1/2}$ and the frequency detuning $\Delta = -20 \times \Gamma$. In Fig. 3, the focal points 1 and 3 actually correspond to the lower and upper branches s_1 and s_3, respectively, in part 1 of Fig. 2(a), whereas the saddle point 2 corresponds to the middle amplitude branch u_2 in part 1 of Fig. 2(a). The hatched areas form a narrow corridor for the upper and stable branch in which the excited electron will eventually fall into the stable state, at focal point 3 in Fig. 3.

4. HIGH-ORDER OPTICAL SUBHARMONIC RESONANCES

The subharmonic excitation of the cyclotron electron at the cyclotron frequency Ω_c can be induced by the optical driving wave at the frequency ω close to the integer multiples of the cyclotron frequency, i.e., $\omega \approx n\Omega_c$. When the subharmonic of the nth order is excited, the momentum of the electron is assumed in the form of Eq. (2.1), where $\Omega = \omega/n$ (n is the order of the subharmonics) [see Fig. 1(b)]. This is the nth-order nonlinear interaction [see also below, Eq. (4.1)], i.e., $N = n$. The dynamics of the cyclotron motion is then governed by Eq. (2.2) with[8]

$$F(R, \rho) = -i[J_{n-1}(n\beta)e^{i\psi}(\rho/R)^n - J_{n+1}(n\beta)e^{-i\psi}(R/\rho)^n]R/\rho^n, \tag{4.1}$$

where J_ν is an ordinary Bessel function of the νth order, $\beta = \rho/\gamma < 1$ is the dimensionless speed of the electron, and ψ is the phase of the driving radiation relative to the center of the cyclotron orbit and can be found in Ref. 5, and $\mu = 3|E|c^2/2e\Omega_0^2$, where E is the electric-field amplitude of the driving wave propagating along the axis x normal to $\mathbf{H}_0$, polarized along the axis y, also normal to $\mathbf{H}_0$. In this case, the expressions for Φ_ρ and Φ_ϕ can be found from Eq. (4.1):

$$\Phi_\rho = -2\mu J_n'(n\beta)\sin(n\phi - \psi),$$
$$\Phi_\phi = -2\mu\beta^{-1}J_n(n\beta)\cos(n\phi - \psi), \tag{4.2}$$

where the prime designates the derivative of $J_n(\zeta)$ with respect to ζ. In the steady-state regimes,[5,8] energy of excitation γ_s is determined through a small detuning, $\Delta_s = \omega/n\Omega_0 - \gamma_s^{-1}$, which in turn is determined as

$$\Delta_s = \pm\Gamma[4J_n^2(n\beta_s)\mu^2/\beta_s^4\gamma_s^2 - \gamma_s^2/G_s^2]^{1/2}, \tag{4.3}$$

where $G_s = \beta_s J_n'(n\beta_s)/J_n(n\beta_s)$. The frequency of subharmonic $\Omega = \omega/n$ follows closely the effective cyclotron frequency $\Omega_c = \Omega_0/\gamma_s$ determined by the relativistic mass effect $m/m_0 = \gamma_s$. For each stable magnitude of energy γ_s, the cyclotron motion can have n equally possible different equidistant states of the phase ϕ_l,

$$\phi_l = \phi_0(n, \mu, \omega) + 2\pi l/n, \qquad \tan(n\phi_0 - \psi) = \Gamma\gamma_s/G_s\Delta_s, \tag{4.4}$$

where l is an integer, $0 \le l < n$. Which of the n stable phase states is excited depends on the initial condition of the excitation. This property is common for any subharmonic oscillations of the nth order regardless of their origin,[12,13] and for second and third subharmonics it is illustrated in Figs. 4 and 5, respectively.

The small-perturbation stability is determined by Eqs. (2.7) with

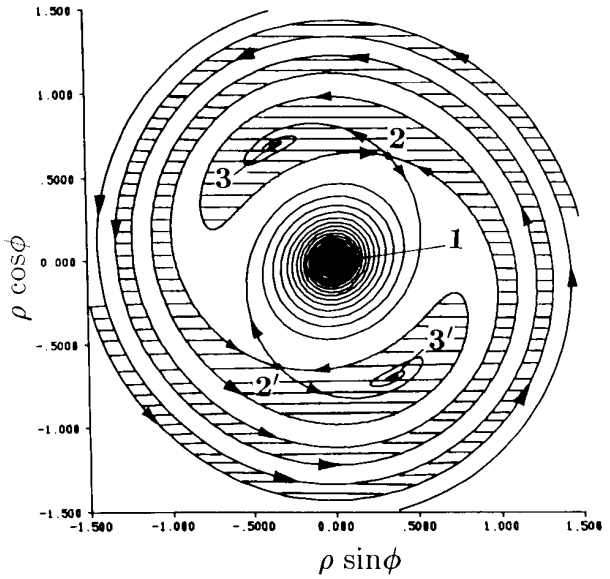

Fig. 4. Phase portrait for the second-order optical subharmonic resonance at the driving amplitude $f = 3.5 \times \Gamma$ and the frequency $\omega/2 \approx 0.8 \times \Omega_0$. Points 1, 3, and 3′ correspond to the stable focal points; points 2 and 2′ corresponds to the unstable saddle points. The hatched areas correspond to the narrow corridors for the respective stable states 3 and 3′.

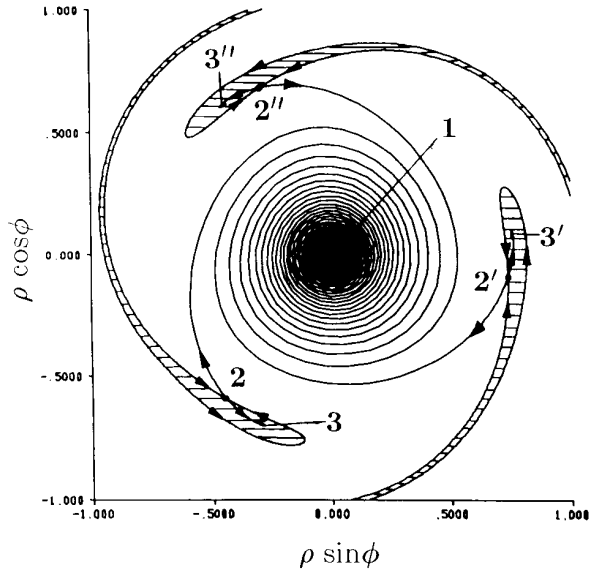

Fig. 5. Phase portrait for the third-order optical subharmonic resonance at the driving amplitude $f = 3.5 \times \Gamma$ and the frequency $\omega/3 \approx 0.8\ \Omega_0$. Points 1, 3, 3′, and 3″ correspond to the stable focal points; points 2, 2′, and 2″ correspond to the unstable saddle points. The hatched areas correspond to the narrow corridors for the respective stables states 3, 3′, and 3″.

$$a_{11} = -2\gamma_s + n/{\gamma_s}^3 G_s, \qquad a_{12} = n\Delta_s\beta_s\gamma_s G_s/\Gamma,$$
$$a_{21} = [(nG_s - {\gamma_s}^2 - 1)\Delta_s - {\beta_s}^2{\gamma_s}^2]/\beta_s{\gamma_s}^3\Gamma, \qquad a_{22} = -n\gamma_s/G_s. \tag{4.5}$$

Using criterion (2.9), one can show that the upper sign in Eq. (4.3) corresponds to stable states and the lower sign to unstable states. The typical results are shown in Fig. 2(b). Specifically, for the second-order subharmonic ($n = 2$), the upper branch and the lower branch [i.e., the zero-amplitude excitation below the lowest cutoff point in part 1 of Fig. 2(b)] always correspond to the stable states, whereas the middle branch between them and the zero-amplitude excitation between the two cutoff points of the upper and middle branches with the axis ω/Ω_0 correspond to the unstable states; see part 1 of Fig. 2(b). For the third-order or higher-order subharmonics ($n \geq 3$), only isolated branches of excitation (isolas) are possible [see part 3 of Fig. 2(b)], and therefore the upper branch for each isola and the zero-excitation branch correspond to stable states; the lower branch for each isola corresponds to the unstable state [see the right-hand curve in part 1 of Fig. 2(b)]. In parts 2 and 3 of Fig. 2(b), the steady-state excitation energy $\gamma_s - 1$ is also depicted versus driving intensity of fixed-frequency detunings. It can readily be seen from the curves in parts 2 and 3 of Fig. 2(b) that again the stable (nonzero-amplitude) branch satisfies the condition $d\gamma_s/d\mu^2 > 0$ (corresponding to the solid curves), whereas the unstable branch satisfies the condition $d\gamma_s/d\mu^2 < 0$ (corresponding to the dashed curves).

The typical phase portraits for the optical subharmonic resonances at the fixed driving amplitude and driving frequency are shown in Figs. 4 and 5. One can see from Figs. 4 and 5 that for the fixed excited momentum amplitude ρ_c, there is more than one steady state of phase, e.g., for $n = 2$, second-order subharmonic, two stable phase states 3 and 3′ and two unstable phase states 2 and 2′ correspond to the single stable and unstable amplitude branches s_3 and s_2, respectively, of the left-hand curve in part 1 of Fig. 2(b). For $n = 3$ (third-order subharmonic) three stable phase states 3, 3′, and 3″ correspond to the stable amplitude branch s_3, whereas three unstable phase states 2, 2′, and 2″ correspond to the unstable amplitude branch s_2 of the right-hand curve in part 2 of Fig. 2(b). For the excitation of the nth-order subharmonic, there are n equally different equidistant states of the phase. This gives rise to the so-called phase multistability[4] similar to that in the generation of subharmonics in other nonlinear systems.[12–14] For the second-order subharmonic, the steady state can be achieved by slowly decreasing the driving frequency across $2\Omega_0$ such that the cyclotron electron will approximately follow the upper (stable) branch of the excited amplitude [see the left-hand curve in part 1 of Fig. 2(b)]. On the other hand, in the case of the third-order (and all the higher orders) subharmonic excitation, only the so-called isolas excitation is possible [see part 3 of Fig. 2(b)]; therefore the steady state of the excited cyclotron electron for $n \geq 3$ can never be obtained by slowly tuning the driving frequency. In order to achieve the excited steady state for $n \geq 3$, an electron has to be excited initially to the significantly high energy. In such a case, the phase of the excitation is crucial, since the electron should be put in one of the narrow corridors in the phase space (see the hatched areas in Fig. 5), which would eventually guide it into the stable steady state.

5. CYCLO-RAMAN OPTICAL RESONANCES

A cyclo-Raman scattering[4,6–8] of the nth order is a process whereby the electron is excited at the cyclotron frequency Ω_c by an optical biharmonic laser with two frequencies ω_1 and ω_2 ($\omega_1 > \omega_2$) such that each one of them is much higher than Ω_c and their difference equals $n\Omega \approx n\Omega_c$, i.e., $\omega_1 - \omega_2 = n\Omega$, where n is an integer [see Figs. 1(c) and 1(d)]. We still choose the configuration in which all the optical traveling waves propagate in the plane normal to $\mathbf{H}_0$ with their polarizations parallel to $\mathbf{H}_0$. In the steady-state regimes, all the energy excitation branches feature multiple isolated branches of excitation (isolas) even for the relatively low energy of the excitation ($\alpha \gtrsim 1$)[6–8]; see, e.g., parts 1 of Figs. 6(a) and 6(b). This feature (a "forced orbit quantization") is peculiar only for the configuration in which the driving waves propagate normally to the dc magnetic field and therefore form a spatially oscillating pattern in the plane of cyclotron motion. The order of the cyclo-Raman excitation coincides with the order of the nonlinear interaction; i.e., again $N = n$. The dynamics of R is governed by Eq. (2.2) with[8]

$$F(R, \rho) = i^{(n+1)}[J_{n-1}(\alpha)(\rho/R)^n - (-1)^n \cdot J_{n+1}(\alpha)(R/\rho)^n]R/\rho^n, \tag{5.1}$$

where $\alpha = \rho(\omega_1 + \omega_2)/\Omega_0$ and $\mu = 3|E_1E_2|c(\omega_1^{-1} + \omega_2^{-1})/16m_0\Omega_0^2$, where $E_{1,2}$ are the electric-field amplitudes of the driving radiations at the frequencies $\omega_{1,2}$, respectively. Although Eqs. (4.1) and (5.1) look quite similar to each other, the significant difference between them is that the upper limit on the argument of the Bessel functions is infinity for the cyclo-Raman resonances and n for the subharmonic res-

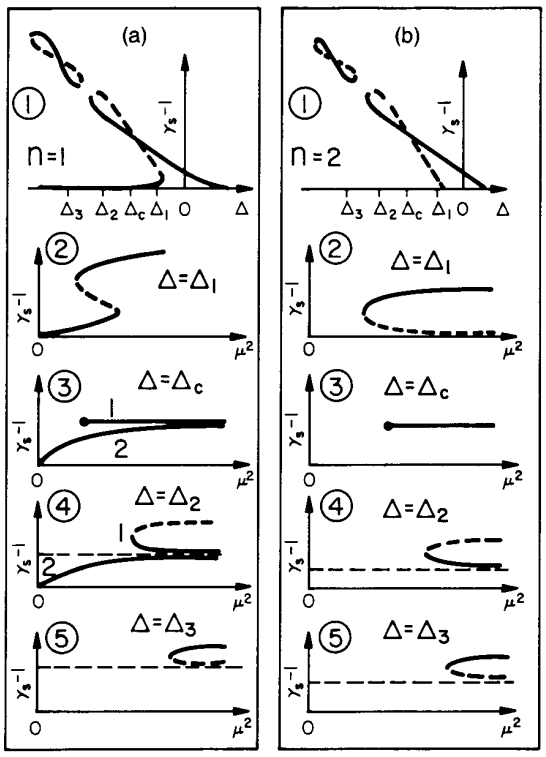

Fig. 6. Curves 1 illustrate the typical hysteretic steady-state excitation as a function of the frequency detuning for the fixed driving amplitude; curves 2–5 illustrate the typical hysteretic steady-state excitation as a function of the driving amplitude for the fixed-frequency detunings for the cyclo-Raman excitation of (a) the first order and (b) the second order. In all cases the solid curves correspond to stable steady states and the dashed curves to unstable ones; the horizontal dashed lines correspond to the lower limit of the excitation.

onances. This [and factor $(-1)^n$ in Eq. (5.1)] makes these two nonlinear processes have somewhat different features. The expression for Φ_ρ and Φ_ϕ can be then found from Eq. (5.1) as

$$\Phi_\rho = \mu Q_+ \sin n(\phi - \pi/2); \Phi_\phi = \mu Q_- \cos n(\phi - \pi/2), \quad (5.2)$$

where $Q_\pm \approx J_{n-1}(\alpha) \pm J_{n+1}(\alpha)$ if $\rho_c \ll 1$.

In th steady-state regime,[7,8] the small detuning $\Delta = \Omega/\Omega_0 - 1$ is determined as

$$\Delta = -\rho_s^2/2 \pm [Q_-(\alpha)/Q_+(\alpha)]\Gamma \sqrt{\mu^2 Q_+^2/\rho_s^2 - 1}. \quad (5.3)$$

For the fixed detuning and intensity of excitation, the nth-order cyclo-Raman resonances (with $n > 1$) exhibit phase multistability essentially similar to phase multistability in the nth-order subharmonics (Section 4); i.e., there are two sets of n equally possible different equidistant states of the phase ϕ^m (m is an integer, $0 \le m < n$) for both the stable and unstable branches:

$$\phi^m = \phi^0 + 2\pi m/n,$$
$$\phi^0 = (n+1)\pi/2n \mp (\tan^{-1}\sqrt{\mu^2 Q_+^2/\rho_s^2 - 1})/n, \quad (5.4)$$

with each set corresponding to one of the signs in ϕ^0 in Eq. (5.4). The minus in Eq. (5.4) corresponds to the amplitude branch with the plus in Eq. (5.3), whereas the plus in Eq. (5.4) corresponds to the amplitude branch with the minus in Eq. (5.3). Again, which of the n stable phase states is excited depends on the initial condition of excitation (see Figs. 4 and 5).

The stabilities of the steady states are determined by Eqs. (2.7) with

$$a_{11} = nQ_-/Q_+ - n - 1,$$
$$a_{12} = n(\Delta + \rho_s^2/2)Q_+\rho_s/Q_-\Gamma,$$
$$a_{21} = -\rho_s/\Gamma + (n - \alpha^2/n - 2Q_-/Q_+)(\Delta + \rho_s^2)Q_+/\rho_s Q_-\Gamma,$$
$$a_{22} = -nQ_-/Q_+. \quad (5.5)$$

Condition (2.9) shows that the amplitude branch with the upper sign in Eqs. (5.3) and (5.4) and the zero-amplitude excitation branch for $n \ge 2$ correspond to stable branches, whereas the amplitude branch with the lower sign corresponds to an unstable branch (see Fig. 6). Figure 6 shows a curious feature of all these regimes, the self-crossing of steady-state amplitude that occurs both in the isolas and in the main "mother" curve. It is unlikely, though, that this feature can be seen in the experiment since one of the self-crossing branches is unstable.

In Fig. 6 the excitation energy $\gamma_s - 1$ is depicted versus the driving intensity at the fixed-frequency detunings for the first-order and second-order cyclo-Raman excitations, where all the dashed curves correspond to unstable states and the solid curves correspond to stable states. One can readily see that the stable steady-state branch also satisfies the criterion $d\gamma_s/d\mu^2 > 0$ for the nonzero excitation ($\gamma_s > 1$) below the self-crossing of each isola excitation and $d\gamma_s/d\mu^2 < 0$ above the self-crossing of each isola. At the self-crossing point, since γ_s = constant with respect to μ [see curves 1 in parts 3 of Figs. 6(a) and 6(b)], $d\gamma_s/\mu^2 = 0$, and one has to distinguish only between stable and unstable phases with the result shown in Eq. (5.4) and the text below it. The phase portraits of the cyclo-Raman resonances show the qualitative similarity to that for subharmonic resonances, for the same order n, respectively.

6. CONCLUSION

We analyzed the stability of the steady-state excitation branches for the nonlinear interaction of a single relativistic cyclotron with optical and microwave radiations. In the main-frequency resonance and subharmonic resonances, the stable amplitude (momentum) branches always satisfy the criterion $d\gamma_s/d\mu^2 > 0$, where $\gamma_s > 1$ is the (dimensionless) energy of the excited electron and μ is the driving amplitude. In the cyclo-Raman resonances, the stable amplitude (momentum) branches satisfy the same criterion below each self-crossing point and the opposite criterion above it. We also explored the nonlinear dynamic behavior of the cyclotron motion in-large, which shows the "corridors of attraction" for steady states and exhibits phase multistability for higher-order processes.

ACKNOWLEDGMENT

This research was supported by the U.S. Air Force Office of Scientific Research.

REFERENCES

1. A. E. Kaplan, "Hysteresis in cyclotron resonance based on weak relativistic-mass effects ofthe electron," Phys. Rev. Lett. **48,** 138–141 (1982).
2. G. Gabrielse, H. Dehmelt, and W. Kells, "Observation of a relativistic bistable hysteresis in the cyclotron motion of a single electron," Phys. Rev. Lett. **54,** 537–539 (1985).
3. A. E. Kaplan, "Hysteretic relativistic resonance of a single electron," Nature **317,** 476–477 (1985); "Ultimate bistability: hysteretic resonance of a slightly-relativistic electron," IEEE J. Quantum Electron. **QE-21,** 1544–1549 (1985).
4. A. E. Kaplan, "Relativistic nonlinear optics of a single cyclotron electron," Phys. Rev. Lett **56,** 456–459 (1986); "Multiphoton excitation of relativistic cyclotron resonance and phase bistability," in *Optical Bistability III*, H. M. Gibbs, P. Mandel, N. Peyghambarian, and S. D. Smith, eds. (Springer, New York, 1985), pp. 240–243.
5. A. E. Kaplan, "Optical high-order subharmonics excitation of free cyclotron electrons," Opt. Lett. **12,** 489–491 (1987).
6. Y. J. Ding and A. E. Kaplan, " 'Isolas' in the three-photon optical excitation of a single cyclotron electron," Opt. Lett. **12,** 699–701 (1987).
7. Y. J. Ding and A. E. Kaplan, "High-order cyclo-Raman scattering of laser by a single electron," Phys. Rev. A **38,** 3109–3112 (1988).
8. A. E. Kaplan and Y. J. Ding, "Hysteretic and multiphoton optical resonances of a single cyclotron electron," IEEE J. Quantum Electron. **QE-24,** 1470–1482 (1988).
9. D. J. Wineland, "Laser-to-microwave frequency division using synchrotron radiation," J. Appl. Phys. **50,** 2528–2532 (1979); see also J. C. Bergquist and D. J. Wineland, "Laser to microwave frequency division using synchrotron radiation II," presented at the 33rd Annual Symposium on Frequency Control, 1979.
10. J. J. Stoker, *Nonlinear Vibrations in Mechanical and Electrical Systems* (Interscience, New York, 1950), Sec. 4.4; see also N. N. Bogoliubov and Yu. A. Mitropolsky, *Asymptotic Methods in the Theory of Nonlinear Oscillations* (Gordon & Breach, New York, 1961); N. Minorsky, *Nonlinear Oscillations* (Van Nostrand, Princeton, N.J., 1962); L. D. Landau and E. M. Lifshitz, *Mechanics* (Pergamon, New York, 1976).
11. C. Hayashi, *Nonlinear Oscillations in Physical Systems* (McGraw-Hill, New York, 1964).
12. A. E. Kaplan, Yu. A. Kravtsov, and V. A. Rylov, *Parametric Oscillators and Frequency Dividers* (Soviet Radio, Moscow, 1966) (in Russian).
13. A. E. Kaplan, "Subharmonic oscillations in a parametric generator with nonlinear capacitance," Radio Eng. Electron. Phys. (USSR) **8,** 1340–1347 (1963); "Anomalous n-th order resonance in single-circuit having a p-n junction with nonlinear capacitance," Radio Eng. Electron. Phys. (USSR) **9,** 1424–1425 (1964); "Contribution to the theory of parametric generator of subharmonics up to n-th order, transient processes," Radio Eng. Electron. Phys. (USSR) **11,** 1214–1221 (1966); "Phase fluctuations in a two-circuit parametric generator of subharmonics," Radio Eng. Electron. Phys. (USSR) **11,** 1354–1359 (1966).
14. A. E. Kaplan, "On generation of high-order subharmonics in the optical range," Radiophys. Quantum Electron. **11,** 900 (1968).
15. L. D. Landau and E. M. Lifshitz, *The Classical Theory of Fields* (Addison-Wesley, Cambridge, Mass., 1971).